LETTERS
PUBLISHED ONLINE: 11 MAY 2014 | DOI: 10.1038/NCLIMATE2235
nature climate change

Evolution of the Southern Annular Mode during the past millennium

Nerilie J. Abram[1,2*], Robert Mulvaney[1], Françoise Vimeux[3], Steven J. Phipps[4], John Turner[1] and Matthew H. England[4]

The Southern Annular Mode (SAM) is the primary pattern of climate variability in the Southern Hemisphere[1,2], influencing latitudinal rainfall distribution and temperatures from the subtropics to Antarctica. The positive summer trend in the SAM over recent decades is widely attributed to stratospheric ozone depletion[2]; however, the brevity of observational records from Antarctica[1]—one of the core zones that defines SAM variability—limits our understanding of long-term SAM behaviour. Here we reconstruct annual mean changes in the SAM since AD 1000 using, for the first time, proxy records that encompass the full mid-latitude to polar domain across the Drake Passage sector. We find that the SAM has undergone a progressive shift towards its positive phase since the fifteenth century, causing cooling of the main Antarctic continent at the same time that the Antarctic Peninsula has warmed. The positive trend in the SAM since ~AD 1940 is reproduced by multimodel climate simulations forced with rising greenhouse gas levels and later ozone depletion, and the long-term average SAM index is now at its highest level for at least the past 1,000 years. Reconstructed SAM trends before the twentieth century are more prominent than those in radiative-forcing climate experiments and may be associated with a teleconnected response to tropical Pacific climate. Our findings imply that predictions of further greenhouse-driven increases in the SAM over the coming century[3] also need to account for the possibility of opposing effects from tropical Pacific climate changes.

Warming of the polar regions has global implications for sea-level rise and climate change feedback processes such as decreased planetary albedo and the release of naturally stored carbon reservoirs. High-latitude amplification of global warming trends is clearly observed across the Arctic[4,5]. In contrast, Antarctica is the only continental region where long-term cooling over the past 2,000 years has not yet been reversed to climate warming[5]. Yet some regions of Antarctica have warmed significantly over the past ~50 years, with the Antarctic Peninsula and parts of west Antarctica displaying the most rapid temperature increases in the Southern Hemisphere[6,7]. Understanding these regional responses of Antarctic temperature to recent climate change requires an improved characterization of natural and anthropogenically driven changes in Southern Hemisphere climate variability.

Here we use the James Ross Island (JRI) ice core from the northern Antarctic Peninsula[7–9] (64.2° S, 57.7° W; Fig. 1), along with other published temperature-sensitive proxies[5], to reconstruct Southern Annular Mode (SAM) variability since AD 1000. The SAM can be defined as the zonal mean atmospheric pressure difference between the mid-latitudes (~40° S) and Antarctica (~65° S; ref 1). The positive phase of the SAM is associated with low pressure anomalies over Antarctica and high pressure anomalies over the mid-latitudes, and this enhanced atmospheric pressure gradient results in strengthening and poleward contraction of the Southern Hemisphere westerly jet stream[1]. The mountainous geographic barrier of the Antarctic Peninsula makes temperature variability in this region particularly sensitive to the strength of the westerly winds passing through Drake Passage. As such, JRI is a key location for documenting SAM-related climate variability (Fig. 1b) and previous work[8,9] has demonstrated that the water-isotope-derived temperature record from the JRI ice core is significantly correlated with observational indices of the SAM[1,10].

The JRI temperature record since AD 1000 has an inverse correlation with the Past Global Changes 2k network (PAGES2k) reconstruction of continental Antarctic temperature[5] (Fig. 1a). This opposing temperature history between the Antarctic Peninsula and the main Antarctic continent is consistent with the spatial response of surface air temperatures to SAM variability (Fig. 1b) and is statistically significant on annual to multidecadal timescales (Table 1). The JRI temperature record also shows similarities to the PAGES2k South American temperature reconstruction[5] that may indicate a shared climate forcing, although the positive correlation between the two data sets is not statistically significant (Table 1). However, in their long-term evolution, the South American and JRI reconstructions both indicate that the coolest 50-year interval of the past millennium occurred at AD 1410–1460, with progressive phases of warming since that time (Fig. 1a).

We combine the JRI temperature record with the PAGES2k compilations of South American and Antarctic temperature-sensitive proxies to derive a weighted composite-plus-scale[11,12] reconstruction of the SAM index during the past millennium (Fig. 2; Methods; Supplementary Table 1 and Figs 1–3). Together, the proxies capture climate information in all seasons and span the mid-latitude to polar domains where the SAM has a major influence on temperature (Fig. 1b). Multimodel climate simulations indicate that the regional temperature patterns associated with modern-day SAM variability persisted through the past millennium (Supplementary Fig. 4), supporting the use of the proxy network to reconstruct the long-term history of the SAM. We restrict the mid-latitude proxy data to the South American continent to produce a reconstruction that is specifically related to SAM variability in the Drake Passage sector. We do this because although the SAM is classically described as a zonally symmetric climate feature, its variability and tropical climate interactions have

[1]British Antarctic Survey, Natural Environment Research Council, Cambridge CB3 0ET, United Kingdom, [2]Research School of Earth Sciences, Australian National University, Canberra, Australian Capital Territory 0200, Australia, [3]Institut de Recherche pour le Développement, Laboratoire HydroSciences Montpellier et Laboratoire des Sciences du Climat et de l'Environment, 91191 Gif-sur-Yvette, France, [4]Climate Change Research Centre and ARC Centre of Excellence for Climate System Science, University of New South Wales, Sydney, New South Wales 2052, Australia. *e-mail: nerilie.abram@anu.edu.au

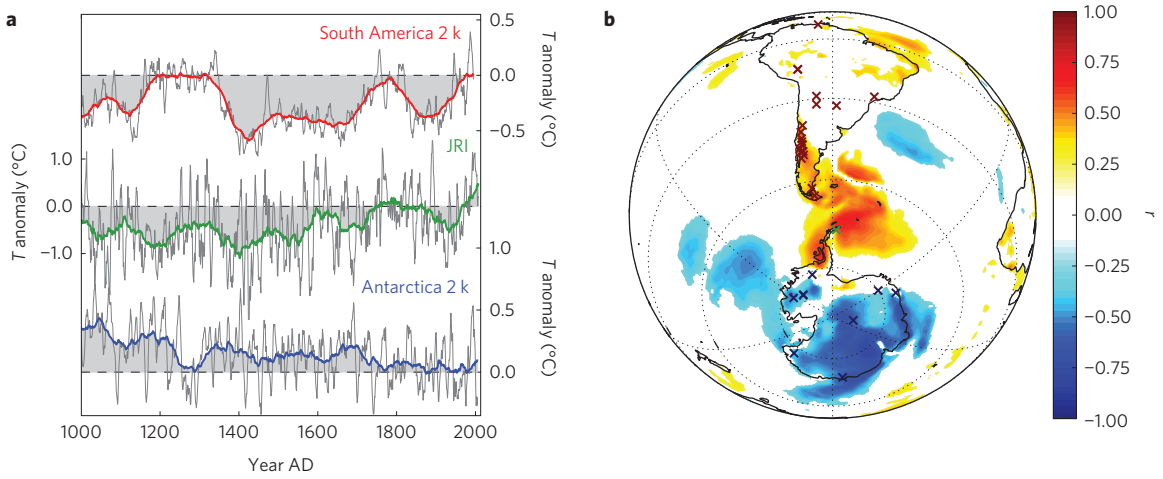

Figure 1 | Regional temperature histories. a, James Ross Island (JRI) temperature reconstruction[7,9] (green) alongside continent-scale temperature reconstructions[5] for South America (red) and Antarctica (blue; excludes JRI). Anomalies shown as 7 yr (thin grey lines) and 70 yr (thick lines and grey shading) moving averages, relative to AD 1961–1990 means (dashed lines). **b**, Location of JRI (green cross) and proxies used in the South America (red crosses) and Antarctica (blue crosses) temperature reconstructions. Shading shows spatial correlation coefficient (r; $p < 0.1$) of the annual SAM index[1] with 2 m air temperature in the ERA-Interim reanalysis[16] (January–December averages; AD 1979– 2012).

seasonal asymmetries that are particularly strong in the South Pacific and Antarctic Peninsula regions[13–15]. Analysis with European Centre for Medium-Range Weather Forecasts Reanalysis data (ERA-Interim)[16] since AD 1979 and climate simulations spanning the past millennium demonstrates, however, that on annual average and longer timescales SAM variability in the Drake Passage sector is highly representative of the circumpolar mean state of the SAM (Supplementary Figs 5 and 6).

Our SAM reconstruction for the past millennium shows that the most extreme negative phase occurred during the fifteenth century (Figs 2c and 3a). Other proxy-based assessments support a minimum in the SAM at this time. For example, an epoch analysis of proxies for Southern Hemisphere circulation identified persistent negative SAM conditions between AD 1300 to 1450[17]. A 600-year reconstruction based on mid-latitude tree growth in New Zealand and South America documented the most extreme negative summer SAM values at ~AD 1470[18] (Fig. 3b) and a 700-year winter sea salt record from the Law Dome ice core also shows a tendency for more positive SAM conditions since ~AD 1500[19]. Similarly, an increase in the frequency of severe droughts in the central Andes over the past six centuries has been attributed to southward contraction of the westerly storm tracks[20] (Supplementary Fig. 7). Together these records demonstrate that the positive trend in the SAM since the fifteenth century is a robust feature that impacted mid-latitude and polar sites around the full SAM domain.

Our reconstruction indicates that the transition to a more positive SAM after the fifteenth century occurred in two stages. First, a progressive increase in the SAM occurred during the ~300 years spanning the sixteenth to eighteenth centuries. This trend then reversed during the nineteenth century, before recommencing in the twentieth century (Fig. 2c). Trend analysis tests on our proxy-based reconstruction indicate that the recent positive trend in the annual SAM index has been significant since ~AD 1940 (Supplementary Fig. 8a).

A valuable tool to assess proxy-model agreement on past SAM behaviour is the Last Millennium transient climate model simulations carried out as part of the fifth Coupled Model Intercomparison Project (CMIP5; refs 21,22; Methods and Supplementary Table 2). The ensemble mean of eight climate models indicates that the positive SAM trend during the twentieth century is a feature that is consistently produced in experiments with transient radiative forcings (Fig. 3c,d). The positive trend in the modelled SAM index since AD 1940 has an equivalent magnitude (+0.3 units per decade) to our proxy-based reconstruction, although the precise initiation point for the twentieth century SAM increase is not as well constrained in the CMIP5 ensemble mean (Supplementary Fig. 8). This is because the CMIP5 simulations do not reproduce the negative SAM trend during the nineteenth century that is observed in the proxy-derived reconstruction. The CMIP5 ensemble mean also shows a much weaker positive trend in the SAM index during the sixteenth to eighteenth centuries (+0.006 units per decade) than indicated by our reconstruction (+0.1 units per decade). Thus, although proxy-model agreement on SAM trends in the twentieth century is reasonably good, there are discrepancies in the structure and magnitude of SAM changes before this time.

The influence of different radiative-forcing mechanisms on the evolution of the SAM is investigated using multiple simulations of the past millennium with a coupled climate model[23] (Methods and Fig. 3e). No long-term trend in the SAM is observed in experiments conducted using only orbital forcing. The addition of anthropogenic greenhouse gases causes a positive shift in the ensemble mean SAM index that exceeds the $+2\sigma$ level of unforced SAM variability during the twentieth century. This is in agreement with other model-based studies that find increased greenhouse gas levels cause a positive shift in the SAM due to enhanced meridional temperature gradients in the Southern Hemisphere[2,3]. It is also consistent with the hypothesis that the early to mid-twentieth-century commencement of Antarctic Peninsula warming is not explained by ozone-forced increases of the SAM alone[9].

The addition of solar forcing to the coupled climate model simulations produces an increasing trend in the SAM index over the sixteenth to eighteenth centuries (Fig. 3e). This could be explained by increasing solar irradiance after the fifteenth century Spörer Minimum, as multimodel assessments of CMIP5 Historical simulations (since AD 1861) have determined that changes in solar irradiance exert a small positive forcing on the SAM (ref. 3). However, the modelled SAM trend during the sixteenth to eighteenth centuries is not significant relative to the distribution of trends in a 10,000-year unforced simulation of the same model. The large pre-industrial trends that are suggested by proxy records may thus imply that the SAM is more responsive to direct solar forcing than indicated by present climate simulations[3], or that the magnitude of solar irradiance changes applied in the Last

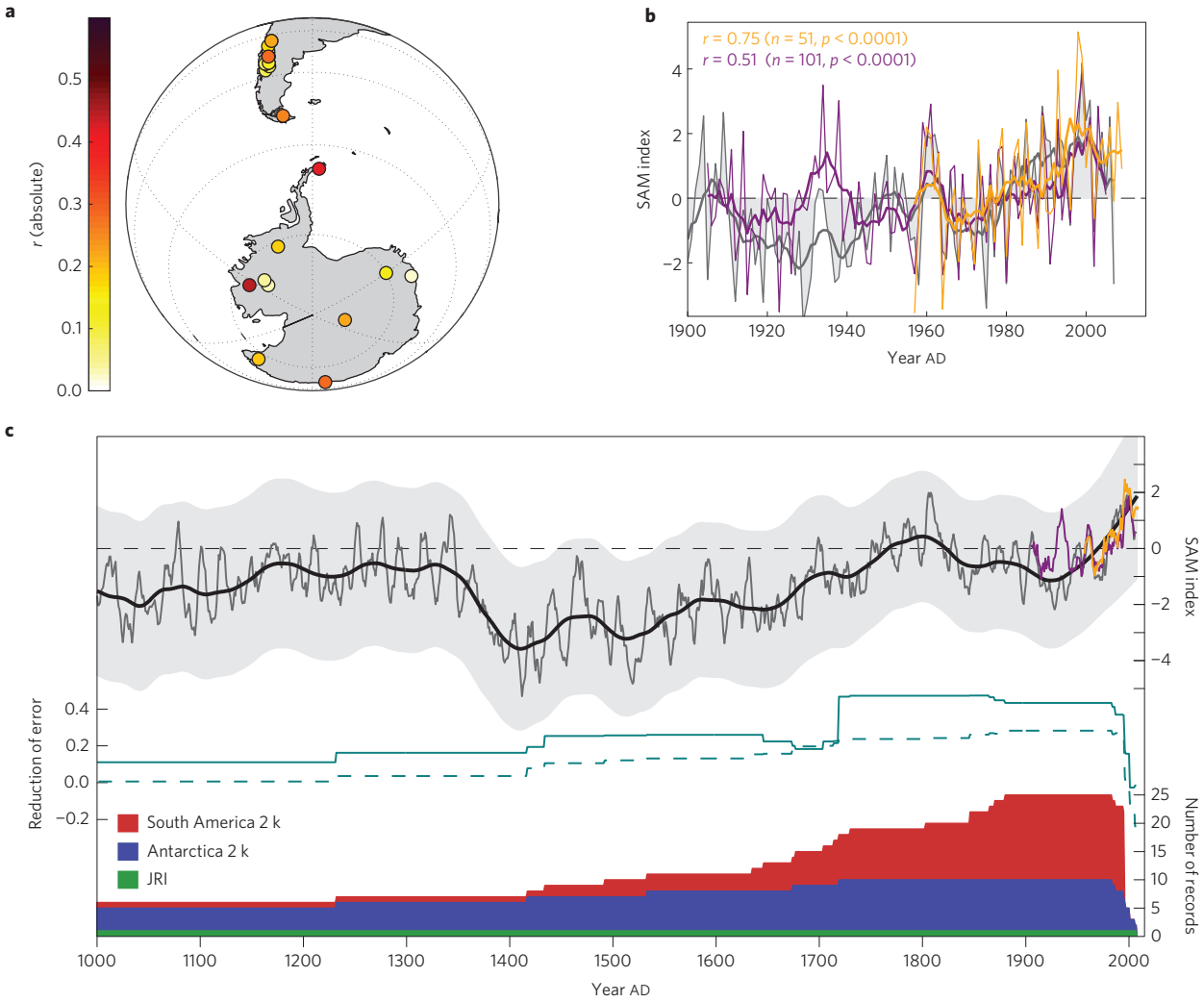

Figure 2 | SAM reconstruction. a, Correlation (*r*) of the proxy network to the annual (January–December) SAM index[1] during AD 1957–1995 calibration interval. **b**, SAM reconstruction (grey lines and shading) alongside Marshall[1] (orange lines; AD 1957–2007) and Fogt[10] (purple lines; AD 1905–2005) SAM indices. All records are shown at annual resolution (thin lines) and 7 yr moving averages (thick lines), relative to AD 1961–1990 mean (dashed line). **c**, SAM reconstruction for the past millennium, as 7 yr moving average (thin grey line) and 70 yr loess filter (thick black line), with 95% confidence interval around the annual reconstruction (grey shading; with 70 yr loess smoothing), relative to AD 1961–1990 mean (dashed black line). Also shown are reduction of error statistics (teal solid line), which remain above RE_{crit} (teal dashed line; $p = 0.05$), the number of contributing proxies and 7 yr moving averages of the Marshall (orange line) and Fogt (purple line) SAM indices.

Millennium simulations is too low[24,25]. Further modelling studies using the full range of solar irradiance change estimates[25] may help to clarify the impact that past solar changes had on the SAM. Alternately, it is possible that proxy-based reconstructions overestimate the magnitude of long-term changes in the SAM, or that trends in the SAM before anthropogenic greenhouse and ozone forcing were caused by internal variability or other physical process that cannot be resolved in radiative-forcing experiments.

The projection of tropically forced climate variability projects on the high-latitude SAM pattern in the Drake Passage sector may provide an additional mechanism to explain SAM trends during the past millennium. Instrumental studies have shown that El Niño–Southern Oscillation (ENSO) variability in the tropical Pacific interacts through a Rossby wave train with storm tracks in the South Pacific, such that El Niño (La Niña) events tend to cause cool (warm) conditions on the Antarctic Peninsula (Fig. 4a) and are associated with negative (positive) SAM states[13–15]. Using a recent multivariate reconstruction of sea surface temperature (SST) in the Niño3.4 region since AD 1150[26], a significant inverse correlation with our SAM reconstruction is obtained (Table 1). It is noted, however, that the Niño3.4 reconstruction also draws on tree growth records from South America. Therefore, we further verify that a significant inverse relationship exists between the Niño3.4 reconstruction and the independent JRI temperature record, located in the core region of ENSO–SAM teleconnections (Fig. 4; Table 1 and Supplementary Fig. 9). This suggests that the association of El Niño with negative SAM states is likely to be a persistent feature of the long-term interaction of these climate modes in the Antarctic Peninsula region.

If the ENSO–SAM relationship that exists on interannual timescales also influences the mean state of these climate modes, then the maximum in Niño3.4 SSTs during the fifteenth century[26] could have contributed to the SAM minimum at this time (Fig. 4b). The positive trend in Antarctic Peninsula temperature and the SAM during the sixteenth to eighteenth centuries, and the reversal of these changes during the nineteenth century, also closely mirror changes in mean Niño3.4 SST. However, tropical Pacific climate seems to become a secondary influence on SAM trends during the twentieth century, when the positive trend in Niño3.4 SST (ref. 26) would be expected to have imposed a negative forcing on the mean state of

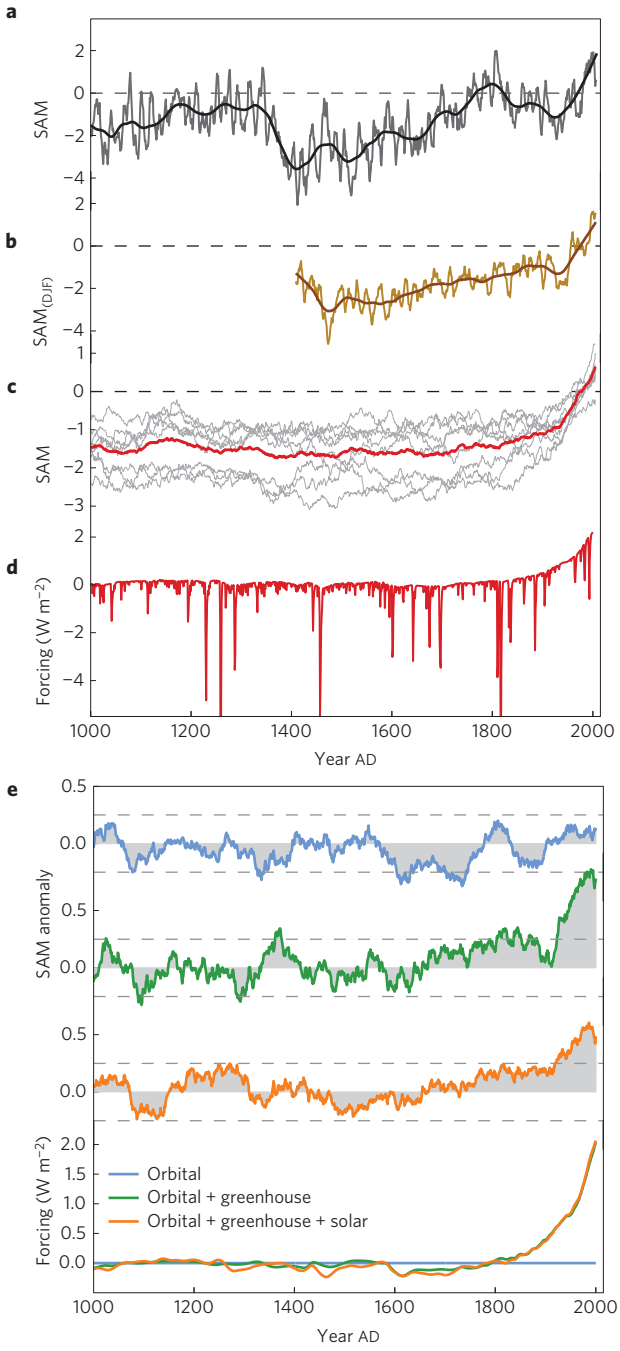

Figure 3 | SAM data–model comparison. a,**b** SAM reconstruction (black line; **a**) compared with a mid-latitude summer SAM reconstruction[18] (brown line; DJF, December–February; **b**); both as 7 yr moving averages (light lines) and 70 yr loess filter (dark lines). **c**, Ensemble mean (red line) SAM index across multimodel CMIP5 simulations[21] (grey lines; 70 yr moving averages). SAM indices (**a**–**c**) relative to AD 1961–1990 means (dashed lines). **d**, Example from CSIRO Mk3L (ref. 23) of using transient radiative forcing[22] applied in Last Millennium simulations (**c**), expressed relative to AD 1001–1200 mean. **e**, CSIRO Mk3L realisations of the SAM index using progressive addition of radiative forcings[23]. Each curve represents the three ensemble average, as 70 yr moving averages relative to AD 1001–1200 means (grey shading). Dashed lines show $\pm 2\sigma$ range of internal variability based on orbital-only simulations.

SAM in the Drake Passage sector. A recent study highlighted that the positive trend in summer SAM during the twentieth century has emerged above the opposing interannual forcing by ENSO (ref. 27).

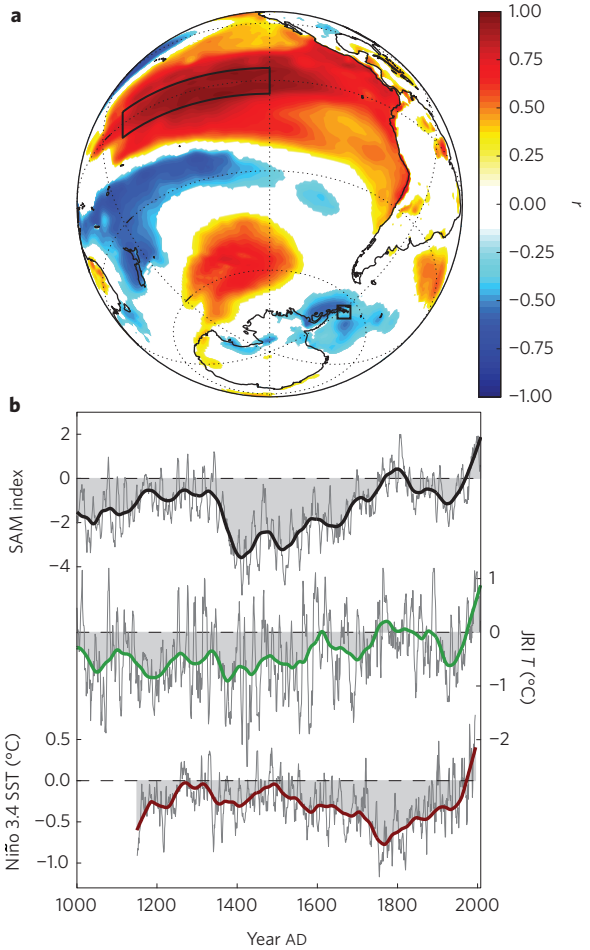

Figure 4 | ENSO teleconnections. a, Spatial correlation coefficient (*r*; January–December averages; AD 1982–2012; $p < 0.1$) of Niño3.4 SST (ref. 30) with ERA-Interim[16] 2 m temperature demonstrating phasing of El Niño (La Niña) states with cooling (warming) in the Antarctic Peninsula region[13]. Black rectangle shows Niño3.4 region, black square shows the location of James Ross Island (JRI). **b**, SAM reconstruction (black line) and JRI temperature (green line), shown alongside a multiproxy reconstruction[26] of Niño3.4 sea surface temperature (SST) (dark red line). All shown as 7 yr moving averages (thin grey lines) and 70 yr loess filter (thick lines and grey shading), relative to AD 1961–1990 means (dashed lines).

Our findings extend this perspective over the past millennium and suggest that tropical Pacific SST trends could have acted in a way that has muted the impact of increasing greenhouse gases and ozone depletion on SAM during the twentieth century.

The long-term mean of the SAM index is now at its highest positive value for at least the past 1,000 years (Fig. 2c). Continued increases in atmospheric greenhouse gases are predicted to force the SAM further towards its positive phase over the coming century[2,3]. At the same time, stratospheric ozone recovery is expected to cause an opposing effect that may limit the magnitude of the positive greenhouse-driven SAM trend in summer[2,3]. However, summer temperatures along the Antarctic Peninsula are already sufficiently high to cause extensive surface ice melt[9], and SAM-driven warming in other seasons may further increase the duration of the melt season in this region[28]. Future greenhouse-driven increases in the SAM are also likely to have implications for limiting warming over continental Antarctica[5] and for southward expansion of the dry subtropical climate belts[18,20]. Furthermore, the tropical Pacific is predicted to experience more extreme El Niño

Table 1 | Correlation statistics for the time series.

Correlation series	Annual averages	7 yr moving averages	70 yr moving averages
JRI temperature versus Antarctica 2 k temperature[5]	$r=-0.055^{*}$ $n=1006$	$r=-0.117^{*}$	$r=-0.535^{\ddagger}$
JRI temperature versus South America 2 k temperature[5]	$r=0.008$ $n=996$	$r=0.075$	$r=0.247$
SAM reconstruction versus Niño 3.4 reconstruction[26]	$r=-0.074^{\dagger}$ $n=846$	$r=-0.163^{\dagger}$	$r=-0.328^{*}$
JRI temperature versus Niño 3.4 reconstruction[26]	$r=-0.077^{\dagger}$ $n=846$	$r=-0.189^{\ddagger}$	$r=-0.379^{*}$

Significance indicated as: $^{*}p<0.1$, $^{\dagger}p<0.05$ and $^{\ddagger}p<0.01$, assessed using 1,000 simulations of AR(1) noise with the same length and lag-1 autocorrelation as the data sets.

events during the coming century[29] and our findings highlight the importance of being able to accurately model how their remote climate teleconnections will also impact the SAM.

Methods

Proxy records. We use the deuterium isotope record from the JRI ice core as a temperature proxy for the Antarctic Peninsula region[8,9]. Full details of the ice core site and isotope analysis can be found in ref. 7. We use the JRI1 age model with annual layer chronology since AD 1807, as in ref. 9. Deuterium isotope measurements made at 10 cm resolution along the upper 300 m of the ice core correspond to better than annual resolution since AD 1111 and were binned to produce annual (~ January–December) averages. The 111 years between AD 1000 and 1110 comprise 85 isotope measurements and interpolation was used to generate a pseudo-annual resolution record over this interval.

We also use temperature-sensitive proxy records for the Antarctic and South America continental regions[5] to capture the full mid-latitude to polar expression of the SAM across the Drake Passage transect. The annually resolved proxy data sets compiled as part of the PAGES2k database are published and publically available[5]. For the South American data set we restrict our use to records south of 30° S and we do not use the four shortest records that are derived from instrumental sources. Details of the individual records used here and their correlation with the SAM are given in Supplementary Table 1.

Data are available at ftp://ftp.ncdc.noaa.gov/pub/data/paleo/icecore/antarctica/james-ross-island/ and http://www.nature.com/ngeo/journal/v6/n5/full/ngeo1797.html

SAM reconstruction. The proxy records from the South America, Antarctic Peninsula and Antarctic continent regions (where SAM has a significant influence on temperature; Fig. 1b) were used to reconstruct an annual average SAM index since AD 1000. We employ the widely used composite plus scale (CPS) methodology[5,11,12] with nesting to account for the varying length of proxies making up the reconstruction. For each nest the contributing proxies were normalized relative to the AD 1957–1995 calibration interval, which represents the interval of maximum overlap between the annual (January–December) Marshall–SAM index (http://www.antarctica.ac.uk/met/gjma/sam.html) and most of the proxy network (Supplementary Table 1). The normalized proxy records were then combined with a weighting[12] based on their correlation coefficient (r) with the SAM during the calibration interval (Supplementary Table 1). The combined record was then scaled to match the mean and standard deviation of the instrumental SAM index during the calibration interval. Finally, nests were spliced together to provide the full 1,008-year SAM reconstruction. Alternate methods for carrying out the CPS reconstruction were explored and the primary findings discussed here are shown to be robust across different methodologies (Supplementary Figs 1 and 2).

For each proxy nest a 95% confidence interval was defined as 1.96 times the standard deviation of the residuals of the SAM reconstruction from the Marshall–SAM index during the calibration interval. The reduction of error statistic was also calculated to test the performance of the reconstruction. The brevity of Antarctic instrumental records limits the ability to cross-validate the SAM reconstruction using separate calibration and verification intervals[18]. Instead, we assess the significance of reduction of error values by repeating 1,000 CPS simulations where the proxy network was replaced by AR(1) time series matching the length and lag-1 autocorrelation of the proxies and we use the upper 95th percentile to determine the critical reduction of error level (RE_{crit}) for each proxy nest. We further verify the SAM reconstruction against the extended Fogt–SAM index[10] (http://polarmet.osu.edu/ACD/sam/sam_recon.html). To carry out this assessment the four seasonal reconstructions were averaged to estimate an annual (December–November) Fogt–SAM index, which was then scaled to match the variance of the Marshall–SAM index from 1961 to 1990.

Model output. We use multimodel output from the subset of CMIP5 climate models that ran transient Last Millennium simulations since AD 850[21,22]. Historical simulations from the same ensemble were used to extend the model output from AD 1850. The CMIP5 Last Millennium and Historical experiments use transient radiative forcings that include orbital, solar, volcanic, greenhouse and ozone parameters as well as land use changes[21,22]. All data was accessed from the Earth System Grid Federation node (http://pcmdi9.llnl.gov/esgf-web-fe/), with the exception of the historical portion of the HadCM3 Last Millennium simulation (provided by A. Schurer, Edinburgh University) and the Commonwealth Scientific and Industrial Research Organisation (CSIRO) Mk3L simulations (ftp://ftp.ncdc.noaa.gov/pub/data/paleo/gcmoutput/phipps2014/). To assess the importance of different radiative-forcing mechanisms, we used multiple simulations of the past 1,500 years carried out with the CSIRO Mk3L coupled climate model, as described in ref. 23. Supplementary Table 2 gives further details on the climate model data sets.

We use monthly resolution mean sea-level pressure fields to calculate the zonal mean at 40° S and 65° S. The model-generated data were averaged into January–December annuals to match the proxy data, normalized relative to the AD 1961–1990 interval and differenced to generate a SAM index[1]. We also use surface air temperature model output to examine SAM–temperature relationships at our proxy sites in the Last Millennium climate simulations (Supplementary Fig. 4).

Data archive. The SAM reconstruction developed here is archived with the World Data Center for Paleoclimatology (http://hurricane.ncdc.noaa.gov/pls/paleox/f?p=519:1:::::P1_STUDY_ID:16197).

Received 2 January 2014; accepted 3 April 2014; published online 11 May 2014

References

1. Marshall, G. J. Trends in the Southern Annular Mode from observations and reanalyses. *J. Clim.* **16,** 4134–4143 (2003).
2. Thompson, D. W. J. *et al.* Signatures of the Antarctic ozone hole in Southern Hemisphere surface climate change. *Nature Geosci.* **4,** 741–749 (2011).
3. Gillett, N. P. & Fyfe, J. C. Annular mode changes in the CMIP5 simulations. *Geophys. Res. Lett.* **40,** 1189–1193 (2013).
4. Screen, J. A. & Simmonds, I. The central role of diminishing sea ice in recent Arctic temperature amplification. *Nature* **464,** 1334–1337 (2010).
5. PAGES 2k consortium Continental-scale temperature variability during the past two millennia. *Nature Geosci.* **6,** 339–346 (2013).
6. Bromwich, D. H. *et al.* Central west Antarctica among the most rapidly warming regions on Earth. *Nature Geosci.* **6,** 139–144 (2013).
7. Mulvaney, R. *et al.* Recent Antarctic Peninsula warming relative to Holocene climate and ice-shelf history. *Nature* **489,** 141–144 (2012).
8. Abram, N. J., Mulvaney, R. & Arrowsmith, C. Environmental signals in a highly resolved ice core from James Ross Island, Antarctica. *J. Geophys. Res.* **116,** D20116 (2011).
9. Abram, N. J. *et al.* Acceleration of snow melt in an Antarctic Peninsula ice core during the twentieth century. *Nature Geosci.* **6,** 404–411 (2013).
10. Fogt, R. L. *et al.* Historical SAM variability part II: Twentieth-century variability and trends from reconstructions, observations, and the IPCC AR4 models. *J. Clim.* **22,** 5346–5365 (2009).
11. Jones, P. D. *et al.* High-resolution palaeoclimatology of the last millennium: A review of current status and future prospects. *The Holocene* **19,** 3–49 (2009).
12. Hegerl, G. C. *et al.* Detection of human influence on a new, validated 1,500-year temperature reconstruction. *J. Clim.* **20,** 650–666 (2007).
13. Ding, Q. H., Steig, E. J., Battisti, D. S. & Wallace, J. M. Influence of the tropics on the Southern Annular Mode. *J. Clim.* **25,** 6330–6348 (2012).
14. Fogt, R. L., Jones, J. M. & Renwick, J. Seasonal zonal asymmetries in the Southern Annular Mode and their impact on regional temperature anomalies. *J. Clim.* **25,** 6253–6270 (2012).
15. Fogt, R. L., Bromwich, D. H. & Hines, K. M. Understanding the SAM influence on the South Pacific ENSO teleconnection. *Clim. Dynam.* **36,** 1555–1576 (2011).
16. Dee, D. P. *et al.* The ERA-Interim reanalysis: Configuration and performance of the data assimilation system. *Q. J. R. Meteorol. Soc.* **137,** 553–597 (2011).

17. Goodwin, I. *et al.* A reconstruction of extratropical Indo–Pacific sea-level pressure patterns during the Medieval Climate Anomaly. *Clim. Dynam.* http://dx.doi.org/doi:10.1007/s00382-013-1899-1 (2013).
18. Villalba, R. *et al.* Unusual Southern Hemisphere tree growth patterns induced by changes in the Southern Annular Mode. *Nature Geosci.* **5,** 793–798 (2012).
19. Goodwin, I. D., van Ommen, T. D., Curran, M. A. J. & Mayewski, P. A. Mid latitude winter climate variability in the south Indian and southwest Pacific regions since AD 1300. *Clim. Dynam.* **22,** 783–794 (2004).
20. Christie, D. A. *et al.* Aridity changes in the temperate-Mediterranean transition of the Andes since AD 1346 reconstructed from tree-rings. *Clim. Dynam.* **36,** 1505–1521 (2011).
21. Taylor, K. E., Stouffer, R. J. & Meehl, G. A. An overview of CMIP5 and the experiment design. *Bull. Am. Meteorol. Soc.* **93,** 485–498 (2012).
22. Schmidt, G. A. *et al.* Climate forcing reconstructions for use in PMIP simulations of the last millennium (v10). *Geosci. Model Dev.* **4,** 33–45 (2011).
23. Phipps, S. J. *et al.* Paleoclimate data-model comparison and the role of climate forcings over the past 1,500 years. *J. Clim.* **26,** 6915–6936 (2013).
24. Shapiro, A. I. *et al.* A new approach to the long-term reconstruction of the solar irradiance leads to large historical solar forcing. *Astron. Astrophys.* **529,** A67 (2011).
25. Schmidt, G. A. *et al.* Climate forcing reconstructions for use in PMIP simulations of the last millennium (v11). *Geosci. Model Dev.* **5,** 185–191 (2012).
26. Emile-Geay, J., Cobb, K. M., Mann, M. E. & Wittenberg, A. T. Estimating central equatorial Pacific SST variability over the past millennium part II: Reconstructions and implications. *J. Clim.* **26,** 2329–2352 (2013).
27. Wang, G. J. & Cai, W. J. Climate-change impact on the 20th-century relationship between the Southern Annular Mode and global mean temperature. *Sci. Rep.* **3,** 2039 (2013).
28. Barrand, N. E. *et al.* Trends in Antarctic Peninsula surface melting conditions from observations and regional climate modelling. *J. Geophys. Res.* **118,** 315–330 (2013).
29. Cai, W. *et al.* Increasing frequency of extreme El Niño events due to greenhouse warming. *Nature Clim. Change* **4,** 111–116 (2014).
30. Reynolds, R. W., Rayner, N. A., Smith, T. M., Stokes, D. C. & Wang, W. An improved *in situ* and satellite SST analysis for climate. *J. Clim.* **15,** 1609–1625 (2002).

Acknowledgements

N.J.A. is supported by a Queen Elizabeth II fellowship awarded by the Australian Research Council (ARC DP110101161). This study contributes to ARC Discovery Project DP140102059 awarded to N.J.A. and R.M. and is part of the British Antarctic Survey's Polar Science for Planet Earth programme financially supported by the Natural Environment Research Council. Modelling work using CSIRO Mk3L was supported by an award to S.J.P. of computational resources on the NCI National Facility through the National Computational Merit Allocation Scheme. M.H.E. is supported by ARC Laureate Fellowship FL100100214. We thank E. Wolff for discussions that improved the paper and we gratefully acknowledge the efforts of the PAGES2k and CMIP5/PMIP3 communities in archiving the proxy synthesis and model products that were used in this study.

Author contributions

N.J.A. conceived the study and carried out the data analysis, with support from the other authors. All authors contributed to the discussion of ideas and writing of the paper.

Additional information

Supplementary information is available in the online version of the paper. Reprints and permissions information is available online at www.nature.com/reprints. Correspondence and requests for materials should be addressed to N.J.A.

Competing financial interests

The authors declare no competing financial interests.